

## Room-temperature InAsSbP/InAs light emitting diodes by liquid phase epitaxy for midinfrared (3–5 $\mu\text{m}$ ) dynamic scene projection

V. K. Malyutenko,<sup>a)</sup> O. Yu. Malyutenko, and A. V. Zinovchuk  
Lashkaryov Institute of Semiconductor Physics, Kiev 03028, Ukraine

(Received 13 July 2006; accepted 6 October 2006; published online 16 November 2006)

The InAsSbP/InAs light emitting diodes (LEDs) grown by liquid phase epitaxy and tuned at several wavelengths inside the 3–5  $\mu\text{m}$  band were tested. Light pattern, radiation apparent temperature ( $T_a$ ), thermal resistance, and self-heating details were characterized at  $T=300$  K in microscale by calibrated infrared cameras operating in the 3–5 and 8–12  $\mu\text{m}$  bands. The authors show that LEDs dynamically simulate very hot ( $T_a \geq 750$  K) targets as well as cold objects and low observable. They resume that low cost LEDs enable a platform for photonic scene projection devices able to compete with thermal microemitter technology. Proposals on how to further increase LEDs performance are given. © 2006 American Institute of Physics. [DOI: 10.1063/1.2390655]

The world of infrared (IR) emitting devices operating in the 3–5  $\mu\text{m}$  wavelength band [midwave IR (MWIR)] is divided into two camps: thermal emitters and photonic devices, such as lasers or light emitting diodes (LEDs). For the last two decades these devices have been increasingly popular because of possible military and commercial applications. Whereas the market of thermal emitters has plateaued, photonic devices have evolved significantly due to recently developed efficient diode lasers that are available for the different wavelengths. While capable of emitting high continuous wave (cw) power [at  $\lambda \sim 4$   $\mu\text{m}$ , quantum-cascade lasers emit 160 mW at 298 K and 1.6 W at 78 K (Ref. 1), and interband cascade lasers at  $\lambda=3.3\text{--}3.6$   $\mu\text{m}$  generate 1.1 W at 78 K (Ref. 2)], the main drawback to these devices is their cost. On the other side, there are strong signs that MWIR LEDs are poised for a potential rebirth. Improving device technology and design has enabled to achieve pulse power output well above 1 mW at room temperature.<sup>3,4</sup> From the short wavelength side, there are devices based on GaSb and InGaAs heterostructures.<sup>5,6</sup> The InAs ternary and quaternary compounds form a basis for the central part of the MWIR, while InSb and HgCdTe LEDs stay at the long wavelength side.<sup>7–10</sup> Thus, conventional LEDs are becoming feasible emitters for unguided long distance communication, long-base “light barrier” devices, MWIR illuminators, and IR countermeasure technologies. By authors’ opinion, the most important application of MWIR LEDs, but one, which is rarely mentioned,<sup>11,12</sup> is that of dynamic infrared scene projection (DISP) devices.

In this letter, we examine whether conventional LEDs can form a platform for photonic MWIR DISP devices that are able to compete with advanced thermal microemitter technology<sup>13</sup> in testing and stimulating IR sensors, including forward-looking IR missile warning systems, IR search-and-track devices, and missile seekers. We also consider how they relate to the laser-based DISP technology, which is worth to be mention even if it is not commercially realized yet. We show that IR LEDs operating at  $T=300$  K have the potential to develop photonic generation of DISP devices capable of simulating not only hot targets (what thermal emitters or lasers can) but cold objects and low observables<sup>14</sup>

as well. We experimentally demonstrate that high performance can be obtained from LEDs grown by liquid phase epitaxy (LPE) which owing to its simplicity and low cost has been used for fabricating heterostructures since the middle 1960s.

Our study is concerned with testing commercially available InAsSbP devices. The LED active regions examined here are grown on 200- $\mu\text{m}$ -thick InAs substrates by LPE as InAsSbP/InAsSb double heterostructures. The benefit of these structures is that the peak-emitting wavelength ( $\lambda_p$ ) can be tailored over the MWIR by merely changing the Sb content in the InAsSb active layer. The chips were packaged into TO-39 case as substrate-down planar ( $450 \times 450$   $\mu\text{m}^2$ ) or substrate-up circular ( $D=300$   $\mu\text{m}$ ) mesa structures. In a planar structure, the top opaque metal contact ( $d=100$   $\mu\text{m}$ ) prevented some of the light from passing through the front emitting surface, reducing the efficiency and power output. On the contrary, the emitting area of a mesa structure was free of contacts as both electrodes are formed on the opposite side of a chip with a 150- $\mu\text{m}$ -diameter central contact (Fig. 1). The points of interest were the uniformity of light and heat in microscale in devices of different geometrical forms and structures. We also wanted to see how the current crowding (CC) effect that prevents LED from having a large emitting area<sup>15</sup> depends on the  $\lambda_p$ . However, our major goal was to measure the apparent temperature of radiation emitted by LEDs that were tuned at different  $\lambda_p$  ( $T_a$  is determined as the temperature of a blackbody emitting equal power in the spec-

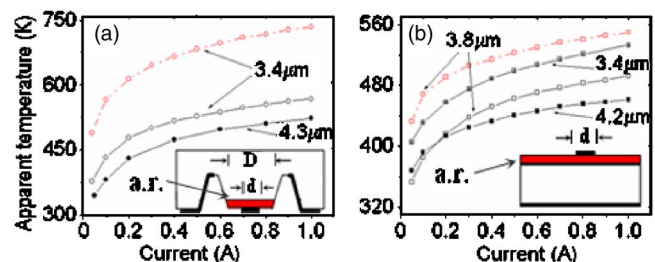


FIG. 1. (Color online) Measured  $T_a$ - $I$  dependencies for mesa (a) and planar (b) LEDs tuned at different  $\lambda_p$ . Dashed lines: narrow-band tests with filter passband  $\Delta\lambda/\lambda_p=8.0\%$  and  $10.5\%$  for  $\lambda_p=3.4$  and  $3.8$   $\mu\text{m}$ , respectively. Solid lines: MWIR-band tests. The insets are schematics of mesa and planar structures with active region (a. r.) shown in red.

<sup>a)</sup>Electronic mail: malyut@isp.kiev.ua

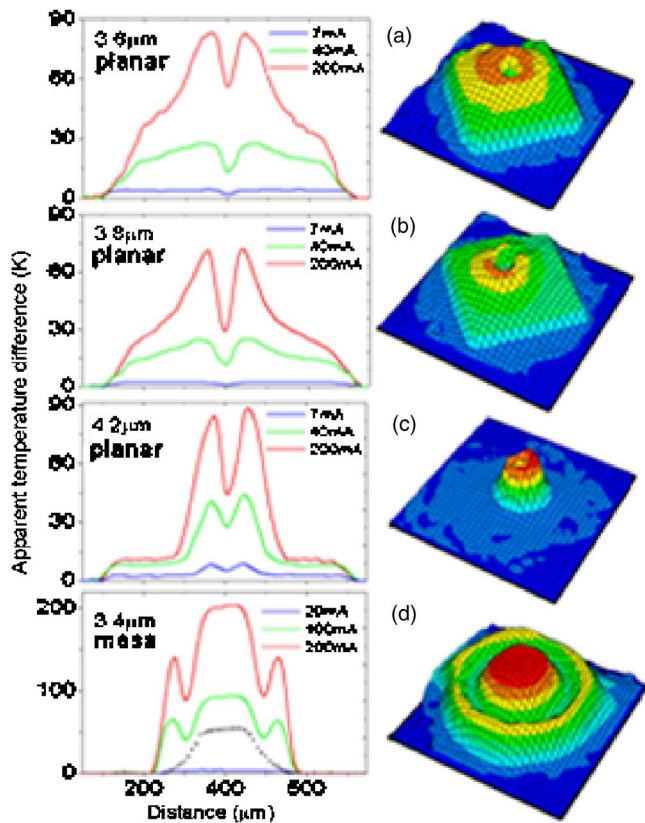


FIG. 2. (Color online) Left column:  $\Delta T_a$  profiles in planar (along the diagonal crossing) and mesa (along the diameter crossing) LEDs at different bias currents. Excess heat profile in the  $3.4 \mu\text{m}$  mesa is shown by the dotted line in tenfold increased vertical scale. Right column: the  $\Delta T_a$  spatial view at  $I=40 \text{ mA}$ .

tral range of interest; it is a thermographic equivalent of light power density).

The light pattern, heat distribution, and  $T_a$  values were characterized by the test system consisting of IR scanning cameras operating in  $3\text{--}5 \mu\text{m}$  (light mapping) and  $8\text{--}12 \mu\text{m}$  (heat mapping) bands in a pulsed mode ( $50 \mu\text{s}\text{--}160 \text{ ms}$  pulse duration) with radiometric (power emitted) and thermographic ( $T_a$  value) calibrations. When equipped with the IR microscope, cameras enable the  $<20 \mu\text{m}$  spatial resolution and the temperature resolution of  $\sim 0.1 \text{ K}$ . Keeping in mind LEDs application in multispectral narrow-band DISP devices, the  $T_a$  measurements with calibrated narrow-bandpass filters matched to spectra of LEDs were also performed. The filter band was about half width at half maximum ( $\Delta\lambda$ ) of the LED spectrum. Due to the specificity of thermographic calibration, the narrow-band  $T_a$  value is higher than MWIR band  $T_a$  and both of these parameters interest users of DISPs.

Figure 1 shows apparent temperature (far-field view) versus current ( $I$ ) dependencies for mesa and planar LEDs tuned at different  $\lambda_p$  and maintained at  $T \sim 300 \text{ K}$ . To minimize overheating of the active area, tests were recorded at current pulse length of  $50 \mu\text{s}$  and repetition rate of  $25 \text{ Hz}$ . As the spatial distribution of radiation was not uniform across the emitting surface (Fig. 2), only “brightest” regions are selected to measure  $T_a$ . The LED output power (not shown) and its equivalent  $T_a$  increase with increasing current, however, the data show that coming from the short wavelength side of MWIR, apparent temperatures of radiation gradually decrease when  $\lambda_p$  increases. This is due to the Auger recom-

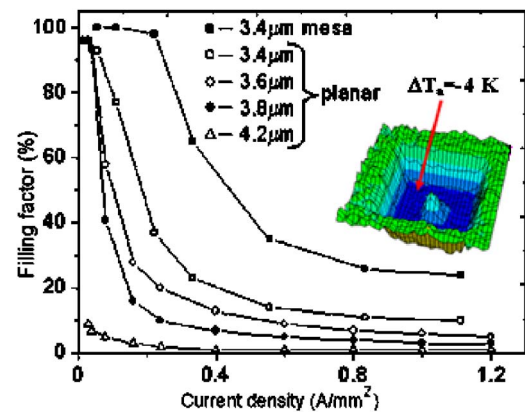


FIG. 3. (Color online) Filling factor as a function of bias current. The inset shows the  $\Delta T_a$  spatial view over the  $3.8 \mu\text{m}$  planar structure at  $I=10 \text{ mA}$ .

ination impact that results in lower quantum efficiency (lower power output and lower  $T_a$  at given  $I$  value) in longer wavelength LEDs. Therefore, only  $3.4 \mu\text{m}$  LEDs demonstrate narrow-band  $T_a$  values compared to those ( $\sim 740 \text{ K}$ ) achieved by thermal emitters.<sup>13</sup> Our tests also have shown that slightly cooled ( $T \sim 200 \text{ K}$ ) LEDs easily step over this limit in cw at  $I \geq 150 \text{ mA}$ .

The single-line ( $400 \mu\text{s}$  pulse duration) profile and two-dimensional distribution ( $160 \text{ ms}$  frame duration) of light on the plane orthogonal to the beam propagation path captured by a microscope that is focused on the  $p\text{--}n$  junction area (near-field view) are shown in Fig. 2 at different  $I$  values. The parameter of interest is the difference between the apparent temperature at a given current and the background  $\Delta T_a = T_a(I) - T_a(0)$ . At a low current, the light pattern is uniform across both planar and mesa active areas. However, increasing current results in a catastrophic decrease of the emitting area in planar structures with top point contact (this contact shadow is clearly seen in figures). More details are shown in Fig. 3 where the filling factor ( $F$ ) of the emitting surface (conditionally determined as the part of an active surface where  $T_a$  values exceed 80% of the maximum) is plotted against the forward current. It is the CC that makes the emitted light to concentrate symmetrically around the top contact and “forget” device geometry. The longer the  $\lambda_p$  smaller the  $F$  value<sup>15</sup> by decreasing from 10% to  $\sim 1.5\%$ . As a result measured at  $I=40 \text{ mA}$  cw, integral power outputs in planar structures were  $24 \mu\text{W}$  ( $3.6 \mu\text{m}$ ),  $21 \mu\text{W}$  ( $3.8 \mu\text{m}$ ), and  $15 \mu\text{W}$  ( $4.2 \mu\text{m}$ ). In mesa structures, CC also decreases the emitting area by  $D^2/d^2$  times ( $F \sim 25\%$ ), but this “crowded” light escapes a structure free of contact shadowing. Further current increase causes an additional nonuniformity in light distribution: two peaks appear at the edges of a mesa with a maximum in between (see also bright ring in the two-dimensional distribution). These satellites originate from the light laterally escaping a mesa and reflecting from its cone (“internal focusing”) and result in  $\sim 20\%$  power output increase. This makes mesa structures a more efficient source for DISP devices.

Recombination losses, Joule losses, CC effect, and low thermal conductivity of III-V’s all contribute to dangerous self-heating of the structure’s center. To get more details on LED heat signature, “thermal” signal measurements were performed with a  $8\text{--}12 \mu\text{m}$  camera with a current pulse duration ( $400 \mu\text{s}$ ) being less than the heat dissipation time

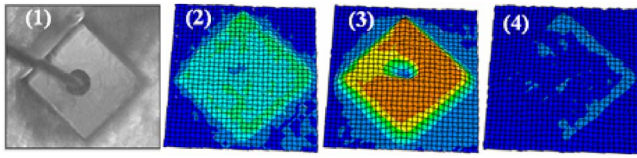


FIG. 4. (Color online) Clearly seen in the visible (1) and slightly seen initially ( $I=0$ ) in the MWIR (2), the  $3.8\ \mu\text{m}$  planar LED can simulate bright target [(3)  $I=10\ \text{mA}$ ] or low observable [(4)  $I=-10\ \text{mA}$ ] when biased.

( $\leq 4\ \text{ms}$ ). As an example, shown in Fig. 2(d) is the heat trap in a mesa structure registered through a substrate at  $I=500\ \text{mA}$ . Due to the possible absorption of thermal radiation by a substrate (free carrier absorption), quantitative temperature tests were problematic. However, a bell-like temperature pattern clearly indicates the region where crowded current flows. The cw tests showed that the thermal resistance (determined as the slope of linear relationship between the junction temperature and drive power) was  $\sim 75\ \text{K/W}$  in most “bright”  $3.4\ \mu\text{m}$  planar LEDs, while it increased up to  $85\ \text{K/W}$  in less efficient  $3.8\ \mu\text{m}$  LEDs. For comparison, in  $3.4\ \mu\text{m}$  mesa this value was  $52\ \text{K/W}$  only that looks like additional benefit of mesa structures.

In the negative luminescence mode,<sup>14</sup> practically all junction areas remain active (see the inset in Fig. 3). It is very important that combining forward and reverse biases evidences a unique IR LED property: the ability to simulate hot and cold targets or low observable with respect to a particular background (Fig. 4). Indeed, as real targets effectively reduce their observability features applying Stealth technologies, modern DISP devices must keep up with synthetic scenarios through projecting target signatures, which are virtually invisible to IR sensors (real-time active camouflage simulation).

To summarize, when it comes to application of LEDs in the DISP technology, difficulties arise from several factors. The nonradiative Auger recombination process and total reflection losses translate into only several percent of external power efficiency. These factors lead to the large electrical power required for operation and cause a device temperature to increase well above the ambient. Low thermal conductivity of ternary-quaternary alloys and heterostructures makes the excess heat difficult to dissipate. Finally, due to unavoidable CC (at forward bias) the noticeable device area of the device becomes practically nonradiative and excess heat generates mostly in region where the current flows, causing local heat trap and dangerous thermal gradients<sup>16</sup> inside a structure. These factors limit room-temperature cw operation of commercial LEDs by simulating  $T_a < 500\ \text{K}$ . Achieving higher temperatures in cw mode demands for moderate cooling.

In the meantime, it has been shown experimentally that LPE IR LEDs (as substrate-up mesa structures) are ideal for use in advanced DISP technology. They allow high-speed ( $>20\ \text{kHz}$ ) simulating high apparent temperature

( $T_a \sim 750\ \text{K}$ ) targets even in structures that are not fully optimized. Being neither monochromatic like a laser nor broadband like a blackbody, LEDs can form a platform for photonic generation of multispectral narrow-band DISP devices operating inside the MWIR band with high spectral output density. For this application, LEDs are better than diode lasers because of their superior stability, less directional nature of light emitted, and lower cost (however, LEDs cannot compete with lasers in the hyperspectral DISP devices). But the major advantage of this technology that significantly improves the present state of the art is the ability to simulate dynamically cold scenes (without cryogenic cooling) and low observable. Even though these power hungry devices exhibit very low external efficiency and suffer from excessive self-heating, they are already very strong contenders in the DISP market. We expect that more efficient light extraction (surface patterning, large-area reflective bottom contact, and intended mesa sidewall profiling), lower power consumption (current spreading, and lower series resistance), and packaging technology with lower thermal resistance can lead to an up to twofold  $T_a$  increase in cw mode. All in all, the results presented can provide the starting point for further device and technology improvement.

<sup>1</sup>J. S. Yu, S. R. Darvish, A. Evans, J. Nguyen, S. Slivken, and M. Razeghi, *Appl. Phys. Lett.* **88**, 041111 (2006).

<sup>2</sup>C. L. Canedy, W. W. Bewley, J. R. Lindle, C. S. Kim, M. Kim, I. Vurgaftman, and J. R. Meyer, *Appl. Phys. Lett.* **88**, 161103 (2006).

<sup>3</sup>V. V. Sherstnev, A. M. Monakhov, A. Krier, and G. Hill, *Appl. Phys. Lett.* **77**, 3908 (2000).

<sup>4</sup>B. Zhurtanov, É. V. Ivanov, A. N. Imenkov, N. M. Kolchanova, A. E. Rozov, N. Stoyanov, and Yu. P. Yakovlev, *Tech. Phys. Lett.* **27**, 173 (2001).

<sup>5</sup>N. D. Stoyanov, B. E. Zhurtanov, A. P. Astakhov, A. N. Imenkov, and Yu. P. Yakovlev, *Semiconductors* **37**, 971 (2003).

<sup>6</sup>B. A. Matveev, M. A. Aydaraliev, N. V. Zotova, S. A. Karandashov, N. D. Il'inskaya, M. A. Remennyi, N. M. Stus, G. N. Talalakin, *IEE Proc.: Optoelectron.* **150**, 356 (2003).

<sup>7</sup>W. W. Bewley, J. R. Lindle, I. Vurgaftman, and J. R. Meyer, *Appl. Phys. Lett.* **83**, 3254 (2003).

<sup>8</sup>T. Ashley, C. T. Elliott, N. T. Gordon, R. S. Hall, A. D. Johnson, and G. J. Price, *Appl. Phys. Lett.* **64**, 2433 (1994).

<sup>9</sup>V. Malyutenko, S. Bolgov, and O. Malyutenko, *Infrared Phys. Technol.* **44**, 11 (2003).

<sup>10</sup>M. K. Haigh, G. R. Nash, N. T. Gordon, J. Edwards, A. Graham, J. Giess, J. E. Hails, and M. Houlton, *Appl. Phys. Lett.* **86**, 011910 (2005).

<sup>11</sup>V. Malyutenko, O. Malyutenko, A. Zinovchuk, N. Zotova, S. Karandashov, B. Matveev, M. Remennyi, and N. Stus, *Sixth International Conference on Mid-Infrared Optoelectronics Material and Devices*, St. Petersburg, Russia, 28 June–2 July 2004, pp. 77–78; <http://www.ioffe.rssi.ru/MIOMD-VI/miomd-abs.html>.

<sup>12</sup>N. N. Naresch C. Das, Kim Olver, F. Towner, G. Simonis, and H. Shen, *Appl. Phys. Lett.* **87**, 041105 (2005).

<sup>13</sup>D. Brett Beasley, Daniel A. Saylor, and Jim Buford, *Proc. SPIE* **4717**, 136 (2002).

<sup>14</sup>V. Malyutenko, *Physica E (Amsterdam)* **20**, 553 (2004).

<sup>15</sup>V. Malyutenko, O. Malyutenko, A. Podoltse, I. Kucheryavaya, B. Matveev, M. Remennyi, and N. Stus, *Appl. Phys. Lett.* **79**, 4228 (2001).

<sup>16</sup>V. Malyutenko, O. Malyutenko, A. Dazzi, N. Gross, and J.-M. Ortega, *J. Appl. Phys.* **93**, 9398 (2003).